Soils and Rocks
An International Journal of Geotechnical and Geoenvironmental Engineering
www.soilsandrocks.com
ISSN 1980-9743
ISSN-e 2675-5475

Numerical analysis of cyclic loading effect on progressive failure of an earth dam upon a multi-laminate framework

Hamzeh Rahimi Dadgar[1#], Mohamad Ali Arjomand[2], Ali Arefnia[1]

Technical Note

Keywords
Earth dam
Progressive failure
Multi-Laminate framework
Cyclic loading

Abstract

In this paper, the progressive failure in an earth dam is evaluated upon a Multi-Laminate framework by considering 10 historical earthquakes in the world, along with their equivalent harmonic cyclic loading. Whenever the framework is given for any suggested plane by direction cosines, it has its certain direction, so, on this basis, the activation order of planes represents the direction and next step of progressive failure. The numerical integration comprises a function that is determined by distributing in sphere area including a radius of one, which can be approximated with several planes, tangential to different points in the sphere area. By calculating numerical integration, the quantity, spread on the sphere, achieved in the aforesaid points to predict fabric anisotropy effects. The framework efficiency is proved by evaluation of removal constants, such as confining pressure, and void ratio. The effects of driven anisotropy studied on all planes of the framework in 10 earthquakes to determine the effects of induced anisotropy on activated and no activated planes, in order to evaluate the progressive failure. Then, the model is capable to predict the coordinate of node of each brick element of the earth dam for next failure.

1. Introduction

Progressive failure appears whereas the average driven resistance, on a sliding surface, is less than the average peak resistance at the time of failure (La Rochelle, 1960). Typical slopes failure appears on any occasion that the strength reduction exceeds in post-peak zones; however, it increases in the driven resistance in the pre-peak parts (Bishop, 1971). This phenomenon causes sudden instability and larger post-failure movements. Some experimental evidence clarified that the average driven resistance is crucial in examining progressive failure (Peck, 1967; Rowe, 1969). A few numerical methods used to analyze cases associated to long slopes (Bernander & Olofsson, 1981; Palmer & Rice, 1973). Part of numerical analyses presented by considering softening phenomena and a non-linear finite element analysis has been performed (Biondi et al., 1976; Prévost & Höeg, 1975).

The analyses express the impact of progressive failure and exhibit various modes of slope and earth dam behavior. Subsequent researches have been carried out to study the issues concerning the progressive failure conditions especially in sand particles by numerical frameworks (Sadrnejad & Labibzadeh, 2006). In this research, the weight coefficient and direction cosines of seventeen planes are calculated using Multi-Laminate theory; the effect of planes is transferred to the middle points of them by numerical integration. Constitutive relations corrected by the method of reducing the number of soil constants, using hypo-plasticity theory (Dafalias, 1986; Dafalias & Manzari, 2004; Manzari & Dafalias, 1997; Taiebat et al., 2010; Wang et al., 1990). Therefore, a constant value at 0.65 is increased by a constant scale used (Halyan, 2001). To determine the number of cycles equivalent to the acceleration of the mappings proposed (Seed & Bruce, 1976), a special method is employed for the time history of shear stress, resulted from the ground motions recorded.

In Multi-Laminate, the equations of the planes and the model constants implemented and calibrated. On each plane the important effects of the applied anisotropy analyzed to evaluate the progressive failure. Evaluating Crack propagation in Earth Dams upon a mixture of Multi-Line technic and Multi-Laminate theory clarified the order of planes activation and progressive failure due to cyclic triaxial test with the same dimensions and boundary conditions and confining pressure for dynamic loading state investigated and compared to laboratory tests (Rahimi Dadgar et al., 2019a, 2019b) and finally the model constants modified based on constitutive relations obtained from elasto-plastic theory (Dashti et al., 2017, 2019).

The major innovative point of this numerical study is that the model is able to predict progressive failure in the earth dam in an equivalent cyclic loading. In this study, to learn the progressive failure, the effect of cyclic loading

#Corresponding author. E-mail: st.h_rdadgar@riau.ac.ir
[1]Islamic Azad University, Roudehen Branch, Department of Civil Engineering, Roudehen, Iran.
[2]Shahid Rajaee Teacher Training University, Department of Civil Engineering, Tehran, Iran.

Submitted on August 13, 2020; Final Acceptance on January 27, 2021. Discussion open until: May 31, 2021.

DOI: https://doi.org/10.28927/SR.2021.056720

is applied. For this purpose, the response spectrum of ten important earthquakes caused serious damages is studied. Then, the aforesaid response ranges, being converted to harmonic charges are studied in numerical method. In this paper, due to the breadth and complexity of earthquake records, as well as the diversity of soil structures' response to each of these applied loads, historical earthquakes and their equivalent cyclic loads at maximum Different ranges, as a factor of the max acceleration of the relevant record, are studied.

2. Materials and method

The numerical relationship between micro-scale behaviors and engineering mechanical properties (macro-scale behavior) due to constitutive equation is the basis of the Multi-Laminate theory. The numerical integration, from a mathematical function, is obtained from sphere area, and the planes are in contact with points of the sphere.

2.1 The framework relations and parameters

The given model has remarkable features and consisting with the principles of advanced soil mechanics. By definition of constitutive relation in the planes and the dilatancy surface and bounding surface and their changes during cyclic loading-unloading and the corresponding match to the critical surface in failure condition, prediction of progressive failure due to order of planes activation is possible. In the following part, governing equations on planes and modifications are considered:

$$G_{(P)} = (2.83-e)^2 / (1+e)\left(\frac{\sigma_{n(P)}}{P_{atm}}\right)^{1/2} G_{0P} P_{atm} \tag{1}$$

$$K_{(P)} = \frac{2(1+v_p)}{3(1-2v_p)} G_{(P)} \tag{2}$$

For determination of critical state line and yield surface, considering the state parameter for all the planes, the following relations used four main surfaces of the numerical applied model at every node of brick elements.

$$e_{c(P)} = e_{0P} - \lambda_{cp}\left(\frac{\sigma_{n(P)}}{P_{atm}}\right)^{\xi_P} \tag{3}$$

$$Cog_{(P)} = \left[\left(Dev_{(P)} - \sigma_{n(P)}\alpha_{(P)}\right) : \left(S_{(P)} - \sigma_{n(P)}\alpha_{(P)}\right)\right]^{1/2} - \sqrt{5/7}\sigma_{n(P)} m_P = 0 \tag{4}$$

$$Dev_{(P)} = \sigma_{(P)} - \sigma_{n(P)} I_{(P)} \tag{5}$$

$$I_{(P)} = \begin{bmatrix} 1 & 0 & 0 \\ 0 & 0 & 0 \\ 0 & 0 & 0 \end{bmatrix} \tag{6}$$

$$r_{(P)} = Dev_{(P)} / \sigma_{n(P)} \tag{7}$$

According to the equation of $Cog_{(P)}$, $L_{(P)}$ and $n_{(P)}$ are obtained as follows:

$$L_{(P)} = \partial Cog_{(P)} / \partial \sigma_{(P)} \tag{8}$$

$$n_{(P)} = \frac{r_{(P)} - \alpha_{(P)}}{r_{(P)} - \alpha_{(P)}} \tag{9}$$

If non-associated flow rule is the dominant plasticity behavior, the following relation used in modeling the progressive failure:

$$R_{(P)} = R'_{(P)} + \frac{1}{3} Di_{(P)} I_{(P)} = B_{(P)} n_{(P)} + C_{(P)}\left(n^2_{(P)} - \frac{1}{3} I_{(P)}\right) + \frac{1}{3} Di_{(P)} I_{(P)} \tag{10}$$

$C_{(P)}$ and $g_{(P)}$ is obtained from the following equations:

$$C_{(P)} = 3.5 \times \frac{(1-C_P)}{C_p} \times g_{(P)} \tag{11}$$

$$g_{(P)} = \frac{2C_P}{5Cos3\theta_{(P)}} \tag{12}$$

The plane dilatiancy is determined by the following relation:

$$Di_{(P)} = A_{d(P)}\left(\alpha^d_{\theta(P)} - \alpha_{(P)}\right) : n_{(P)} \tag{13}$$

The dilatancy surface is defined as follows:

$$\alpha^d_{\theta(P)} = 0.8 \times \left[g_{(P)} \times M_P \times exp\left(n^d_P \times \psi_{(P)}\right)\right] n_{(P)} \tag{14}$$

The cyclic loading parameter is defined as the following relation:

$$CLP_{(P)=}\left(3 \times G_{(P)} n_{(P)} : de_{(P)} - n_{(P)} : r_{(P)} d\varepsilon_{V(P)} \times K_{(P)}\right) / (K_{P(P)} + 2G_{(P)}\left(B_{(P)} + C_{(P)} trn^3_{(P)}\right) - K_{(P)} Di_{(P)} n_{(P)} : r_{(P)}) \tag{15}$$

Whereas, the elastic deviatoric strain is determined by the following equation:

$$de^e_{(P)} = ds_{(P)} / \left(2G_{(P)}\right) \tag{16}$$

The framework plastic coefficient is calculated as follows:

$$K_{P(P)} = 0.8 \times \sigma_{n(P)} \times h_{(P)}\left(\alpha^b_{\theta(P)} - \alpha_{(P)}\right) : n_{(P)} \tag{17}$$

2.2 Equivalent cyclic loading

Considering earthquake acceleration record, Fourier spectrum, and the equivalent harmonic load of ten important earthquakes, according to the number of equivalent cycles offered for different magnitudes, the highest equivalent cycle obtained in each range is selected as the number of cycles, equivalent to its characteristic. Frequency content is so effective on obtained equivalent cyclic load and consequently, number of equivalent cycles determines by considering Fourier amplitude. According to the Fourier spectrum of the selected earthquake recordings, it was observed that high duration with closed frequency content causes fewer equivalent cycles than low duration with open frequency content. Equivalent cyclic load specifications of earthquakes with different range of magnitude, fore earthquake

with magnitude of 6-6.5, and N considered equal to 0.45 and 10 respectively, and for earthquake with magnitude of 6.5-7, C_{eq} and N considered equal to 0.65 and 15 orderly, and finally fore magnitude of 7-8, C_{eq} considered equal to 0.75 and chosen N is 20. The characteristics of earthquake records of Chichi, Tabas, Kocaeli, Duzce, Northridge, Loma Prieta, Kobe, Imperial Valley, Palm Spring and Whittier used development of the model for purpose of progressive failure occurrence evaluation due to seismic excitation.

2.3 Earth dam modeling

Roudbar-Lorestan earth dam is located at 32.9032° N, 49.6833° E, in western Iran. This earth dam is located on the Roudbar River, a tributary of the East Dez River, about 511 km south of Aligudarz city in Lorestan province and the Zagros Mountain. Some technical specifications of the ECRD dam body are normal water level of 1756 m, and dam crest level of 1766 m above sea level, crest length of 185 m, crest width of 15 m, earth dam height of 153 meters, tunnel overflow, average annual flow of 30.2 cubic meters per second, maximum monthly flow of 250.5 cubic meters per second and minimum monthly flow of 4.1 cubic meters per second. Zones used for the analysis of Roudbar-Lorestan earth dam based on 16 layer construction modeling are shown in Figure 1.

The parameters of the materials of the earth dam are given in Table 1. 8-point brick elements are used for analysis. The structure has 570 elements and 1260 nodes. It is assumed that the earth dam foundation is solid, so the nodes on the base are considered to be fixed.

3. Results

Based on mathematical relations mentioned and material properties of the earth dam and boundary conditions and finite element method relations and standard brick element used and layers of construction considered, and equivalent cyclic loading of earthquake spectrums, the Multi-Laminate constants used in the evaluation of progressive failure is 110 for G_0^p, 0.4 for v_P, 0.65 for M_P, 0.85 for C_P, 0.02 for λ_{CP}, 1.05 for e_{0P}, 0.78 for ξ_P, 0.03 for m_P, 4 for h_{0P}, 0.9 for C_{hP}, 1.1 for n_P^d, 0.5 for A_{0P}, and 3.5 for n_P^d. Using the failure point coordinates and prediction of next failure point by the framework, progressive failure evaluated in full reservoir state of the dam. Progressive failure, due to seismic excitation by earthquake with magnitude of 7 to 8,and considering 5, 10, 15 and 20 as N, illustrated in Figures 2 to 5.

4. Discussion

In high-magnitude earthquakes, the exciting frequency content had high amplitude over an extensive rate of frequencies. However, the higher the energy level, the higher the number of cycles equivalent to an earthquake, and depending on the prevailing period of the studied soil barrier, it will be able to create larger deformations. In the range of plastic strains, the number of cycles affects the decrease and increase of

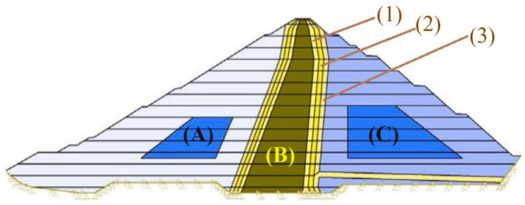

Figure 1. Construction layers and Zones of the earth dam.

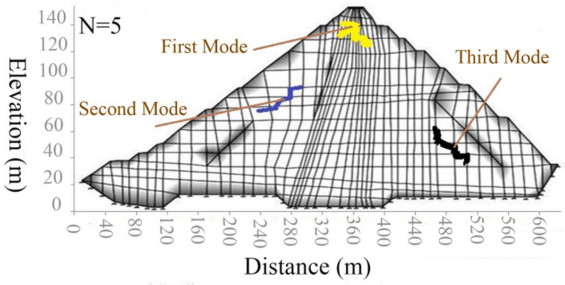

Figure 2. First step of progressive failure.

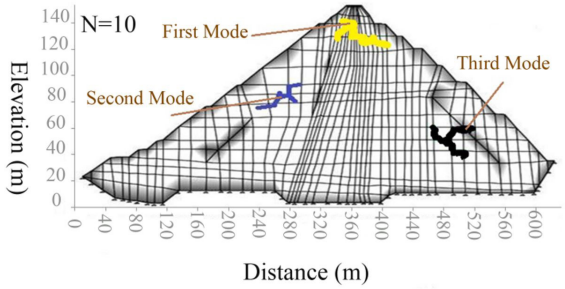

Figure 3. Second step of progressive failure.

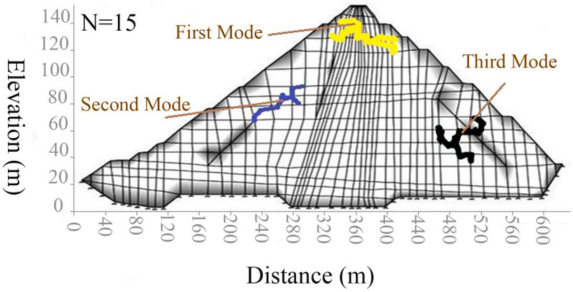

Figure 4. Third step of progressive failure.

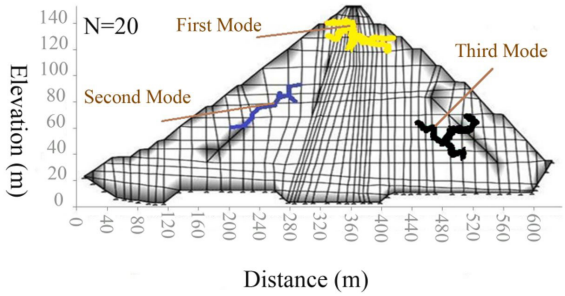

Figure 5. Fourth step of progressive failure.

Table 1. Parameters of Roudbar-Lorestan earth dam materials.

Material Description of Zones	v	E	γ_{dry}	γ_{wet}	γ_{sat}	C'	$\varnothing'$	Hydraulic Conductivity
		kPa	kN/m^3	kN/m^3	kN/m^3	kPa	(°)	(cm/sec)
Upstream- (A)	0.25	70	21.5	22.5	23.5	0	45	1.0×10^{-1}
Impervious Core- (B)	0.35	35	21.5	23.1	23.4	50	25	1.0×10^{-6}
Downstream Rock fill-(C)	0.25	70	21.0	22.0	23.0	0	45	1.0×10^{-1}
Fine Filter-(1)	0.33	70	19.0	20.0	21.9	0	37	5.0×10^{-4}
Drainage Transition-(2)	0.25	70	21.0	22.0	23.2	0	45	1.0
Coarse Filter-(3)	0.30	70	19.5	20.5	22.2	0	39	5.0×10^{-2}
Random Rock fill	0.25	50	20.5	21.5	22.9	0	42	1.0×10^{-2}

plastic modules and as the number of cycles increases, their rate of change will also increases. According to the Fourier transform of selected earthquake records, it was observed that the number of harmonic load cycles equivalent to earthquake records depends on the frequency content and the time of its continuation. High continuity time with closed frequency content causes lower number of equivalent cycles compared with low duration mode with open frequency content.

The acceleration coefficients and the number of equivalent cycles are 0.45, 10, plus 0.65, 15, which are respectively compliant to the earthquake Magnitude at 6-6.5 and 6.5-7 on (the Richter scales). Furthermore, the number of cycles compliant to earthquakes Magnitude at 7-8 (Richter scales) is 20 and its acceleration coefficient is 0.75 respectively. In the study of progressive failure, it is found that among the three main modes of failure that are considered upstream, downstream, and the crest of the earth dam, the first mode is related to the crest of earth dams. Progressive failure at Roudbar-Lorestan earth dam in earthquakes with magnitudes of 6 to 6.5 and also 6.5 to 7 Richter, does not leading to the formation of the failure surface. However, in earthquakes with a magnitude of 7 to 8 Richter, with increasing step-by-step harmonic load cycle, wedge rupture is formed in the crest of the dam, and according to the results of numerical modeling, the rupture is more likely due to the progress of cracks in the dam crest.

5. Conclusion

Achieving a reliable numerical method to evaluate the progressive failure of earth dams due to seismic excitation has always been a challenging target for geotechnical engineers. For solving this problem, Conversion of seismic spectra to equivalent harmonic loads and their application to the desired earth dam and evaluation the surface of rupture created and the consequent progressive failure is so considerable. The Multi-Laminate framework basis is the calculating the numerical relationship between micro-scale behaviors and engineering mechanical properties in constitutive equations. So, the framework was chosen because of its high accuracy and calibrated by the most reliable previous numerical and experimental researches. By considering 10 main historical earthquakes in the world, and their equivalent harmonic loading and the related factors, the purpose of the research was implemented.

Finite Element Method Considering directional cosines and weight coefficient of 17 planes and constant parameters related to elasticity, plastic modulus, critical state line and yield surface in each plane led to the correct diagnosis of progressive failure. A magnitude 7 earthquake struck on November 12, 2017 at 18:18 UTC, in Ezgeleh, Iran. As a result of this earthquake, Roudbar-Lorestan earth dam was also damaged, due to which the failure surface was propagated resulting in the progressive failure, with a behavior similar to the 3 main modes of damage predicted in full reservoir state of the dam in this paper. Although Ezgeleh earthquake record is not mentioned in 10 historical earthquakes of this study, it is worth mentioning, the progressive failure caused by this earthquake at 7.3 Magnitude showed a failure compatible to what the numerical analysis predicted in Figure 5, and the critical major rupture occurred on the crest of the dam considering that the rupture was 140 m high from the foundation and the movement was towards downstream. In 2 other failure modes, the behavior of the dam was similar to the behavior, predicted by numerical modeling through a Multi-Laminate framework. The numerical method used in this research can be used as a remarkable method for rapid and reliable evaluation to detect progressive failure due to seismic excitation in future geotechnical researches.

Declaration of interest

The authors have no conflicts of interest to declare. All co-authors have observed and affirmed the contents of the paper and there is no financial interest to report. We

assure that the paper is original and is not under review at any other Journal.

Author's contributions

Hamzeh Rahimi Dadgar: Conceptualization, Data Curation, Methodology, Validation. Mohamad Ali Arjomand: Supervision. Ali Arefnia: Project Administration.

References

Bernander, S., & Olofsson, I. (1981). On the formation of progressive failure in slopes. In *Proceedings of the 10th International Conference of Soil Mechanics and Foundation Engineering* (pp. 357-362). Stockholm: Balkema.

Biondi, P., Manfredini, F., Martinetti, S., Rickbackhi, R., & Riccioni, R. (1976). Limit load of a foundation in a strain-softening soil. In *Proceedings of the International Conference on Numerical Methods in Geomechanics* (pp. 591-596). Blacksburg: ASCE.

Bishop, A.W. (1971). The influence of progressive failure on the choice of the method of stability analysis. *Geotechnique*, 21(2), 168-172. https://doi.org/10.1680/geot.1971.21.2.168.

Dafalias, Y.F. (1986). Bounding surface plasticity. I: mathematical foundation and hypoplasticity. *Journal of Engineering Mechanics*, 112(9), 966-987. https://doi.org/10.1061/(ASCE)0733-9399(1986)112:9(966)

Dafalias, Y.F., & Manzari, M.T. (2004). Simple plasticity model accounting for fabric changes effect. *Journal of Engineering Mechanics*, 130(6), 622-634. http://dx.doi.org/10.1061/(ASCE)0733-9399(2004)130:6(622).

Dashti, H., Sadrnejad, S. A., & Ganjian, N. (2019). A novel semi-micro multilaminate elasto-plastic model for the liquefaction of sand. *Soil Dynamics and Earthquake Engineering*, 124, 121-135. https://doi.org/10.1016/j.soildyn.2019.05.031.

Dashti, H., Sadrnejad, S.A., & Ganjian, N. (2017). Modification of a constitutive model in the framework of a multilaminate method for post-liquefaction sand. *Latin American Journal of Solids and Structures*, 14(8), 1569-1593. http://dx.doi.org/10.1590/1679-78253841.

Halyan, M. (2001). Fully coupled earthquake response analysis of earth dams using a critical state sand model. *International Journal of Seismic Design*, 1(3), 23-31.

La Rochelle, P. (1960). *The short term stability of slopes in London Clay*. University of London.

Manzari, M.T., & Dafalias, Y.F. (1997). A critical state two-surface plasticity model for sands. *Geotechnique*, 47(2), 255-272. http://dx.doi.org/10.1680/geot.1997.47.2.255.

Palmer, A.C., & Rice, J.R. (1973). The growth of slip surfaces in the progressive failure of overconsolidated clays. *Royal Society of London*, 332(1591), 527-548. https://doi.org/10.1098/rspa.1973.0040.

Peck, R.B. (1967). Stability of natural slopes. *Journal of the Soil Mechanics and Foundations Division*, 93(4), 403-417.

Prévost, J.H., & Höeg, K. (1975). Soil mechanics and plasticity analysis of strain softening. *Geotechnique*, 25(2), 279-297. http://dx.doi.org/10.1680/geot.1975.25.2.279.

Rahimi Dadgar, H., Arjomand, M.A., & Arefnia, A. (2019a). Crack Detection in Earth Dams upon a Multiline-Multilaminate Model. *IACSIT International Journal of Engineering and Technology*, 11(3), 445-455. http://dx.doi.org/10.21817/ijet/2019/v11i3/191103030.

Rahimi Dadgar, H., Arjomand, M.A., & Arefnia, A. (2019b). Numerical analysis of cyclic loading effect on progressive failure in earth dams upon a multiline-multilaminate model. *IACSIT International Journal of Engineering and Technology*, 11(3), 492-504. http://dx.doi.org/10.21817/ijet/2019/v11i3/191103038.

Rowe, P.W. (1969). Progressive failure and strength of a sand mass. In *Proceedings of the 7th international Conference of Soil Mechanics and Soil Foundations Engineering* (pp. 341-349). Mexico: ISSMGE.

Sadrnejad, S.A., & Labibzadeh, M. (2006). A continuum/discontinuum micro plane damage model for concrete. *International Journal of Civil Engineering*, 4(4), 296-313.

Seed, H.B., & Bruce, R. (1976). Stabilization of potentially liquefiable sand deposit using Gravel Drain System. *Earthquake Engineering Research Journal*, 2(4), 104-111.

Taiebat, M., Jeremić, B., Dafalias, Y.F., Kaynia, A.M., & Cheng, Z. (2010). Propagation of seismic waves through liquefied soils. *Soil Dynamics and Earthquake Engineering*, 30(4), 236-257. http://dx.doi.org/10.1016/j.soildyn.2009.11.003.

Wang, Z., Dafalias, Y.F., & Shen, C. (1990). Bounding surface hypoplasticity Model for Sand. *Journal of Engineering Mechanics*, 116(5), 983-1001. http://dx.doi.org/10.1061/(asce)0733-9399(1990)116:5(983).

List of Symbols and Acronyms

$A_{d(P)}$: Dilatancy Constant of the framework

C' : Cohesion Parameter

C_{eq} : Equivalent Acceleration Coefficient

$CLP_{(P)}$: Cyclic loading Plastic coefficient

$Cog_{(P)}$: Cone geometry in the deviatoric stress space of the plane

$Dev_{(P)}$: Deviatoric stress tensor in the plane

$Di_{(P)}$: Dilation parameter for the plane

$de^{e}_{(P)}$: Elastic deviatoric strain

E: Elasticity Modulus

ECRD: Earth Core rockfill Dam

e: Void ratio

$e_{c(P)}$: Critical void ratio

$G_{(P)}$: Elastic shear modulus

G_0^P, v_P : Model Constants in plane related to elasticity

$g_{(P)}$: Interpolation function for stress path

h_{0P}, C_{hP}, n_P^b: Model Constants in plane related to plastic modulus

$K_{(P)}$: Elastic bulk modulus

$K_{P(P)}$: Framework plastic coefficient

$L_{(P)}$: Yield surface gradient in space

$M_P, C_P, \lambda_{CP}, e_{0P}, \xi_P$: Model Constants in plane related to critical state

m_P : Model Constant in plane related to yield surface

N: Number of Equivalent Cycles

$S_{(P)}$: Deviatoric stress parameter

$n_{(P)}$: Tensor perpendicular to the yield surface

P_{atm} : Atmospheric pressure

R_P : Direction vector

$R'_{(P)}$: Deviatoric part of R_P

$r_{(P)}$: Stress ratio tensor in the plane

$\alpha_{(P)}$: Deviatoric back stress ratio tensor

$\alpha^{d}_{\theta(P)}$: Dilatancy surface

γ_{dry} : Dry unit weight

γ_{wet} : Wet unit weight

γ_{sat} : Saturated unit weight

θ : Angle of Orientation

v : Poisson's ratio

$\sigma_{n(P)}$: Normal stress in plane

$\varnothing'$: Drained angle of internal friction

ψ_P : Dilatancy parameter of the plane